Available online at www.sciencedirect.com

ScienceDirect

Geochimica et Cosmochimica Acta 194 (2016) 310–324

Geochimica et Cosmochimica Acta

www.elsevier.com/locate/gca

Stable isotope variations ($\delta^{18}O$ and δD) in modern waters across the Andean Plateau

John Bershaw [a,*], Joel E. Saylor [b], Carmala N. Garzione [c], Andrew Leier [d], Kurt E. Sundell [b]

[a] *Portland State University, Portland, OR, USA*
[b] *University of Houston, Houston, TX, USA*
[c] *University of Rochester, Rochester, NY, USA*
[d] *University of South Carolina, Columbia, SC, USA*

Received 16 December 2015; accepted in revised form 7 August 2016; Available online 13 August 2016

Abstract

Environmental parameters that influence the isotopic composition of meteoric water ($\delta^{18}O$ and δD) are well characterized up the windward side of mountains, where orographic precipitation results in a predictable relationship between the isotopic composition of precipitation and elevation. The topographic and climatic evolution of the Andean Plateau and surrounding regions has been studied extensively by exploiting this relationship through the use of paleowater proxies. However, interpretation on the plateau itself is challenged by a poor understanding of processes that fractionate isotopes during vapor transport and rainout, and by the relative contribution of unique moisture sources. Here, we present an extensive dataset of modern surface water samples for the northern Andean Plateau and surrounding regions to elucidate patterns and causes of isotope fractionation in this continental environment. These data show a progressive increase in $\delta^{18}O$ of stream water west of the Eastern Cordillera (~1‰/70 km), almost identical to the rate observed across the Tibetan Plateau, attributed to a larger fraction of recycled water in precipitation and/or increased evaporative enrichment downwind. This may lead to underestimates of paleoelevation, particularly for sites deep into the rainshadow of the Eastern Cordilleran crest. That said, elevation is a primary control on the isotopic composition of surface waters across the entire Andean Plateau and its flanks when considering the most negative $\delta^{18}O$ values, highlighting the need for sufficiently large datasets to distinguish minimally evaporated samples. There is a general increase in $\delta^{18}O$ on the plateau from north to south, concomitant with an increase in aridity and decrease in convective moistening (amount effect). Lastly, stable isotope and seasonal precipitation patterns suggest easterlies provide the vast majority of moisture that falls as precipitation across the Andean Plateau and Western Cordillera, from Peru to northern Bolivia (−13° to −20° latitude), with Pacific-derived moisture contributing a minor amount at low elevations near the coast.

Keywords: Stable isotope geochemistry; Meteoric water; South America; Andes; Altiplano; Climate; Paleoaltimetry

1. INTRODUCTION

Modern stable isotope variation in precipitation is fairly well-understood for the windward side of mountains where $\delta^{18}O$ and δD have been shown to be inversely related to elevation (Garzione et al., 2000; Gonfiantini et al., 2001;

* Corresponding author. Fax: +1 503 725 3025.
E-mail address: bershaw@pdx.edu (J. Bershaw).

http://dx.doi.org/10.1016/j.gca.2016.08.011
0016-7037/

Poage and Chamberlain, 2001). This relationship has been exploited for paleoaltimetry studies where various proxies for precipitation are used in the rock record to estimate the timing of topographic growth (or decay) for many of the world's mountain ranges and plateaux (Bershaw et al., 2010; Currie et al., 2016; Kar et al., 2016; Kent-Corson et al., 2009; Leier et al., 2013; Mulch, 2016; Mulch et al., 2006; Rowley and Garzione, 2007; Saylor and Horton, 2014; Saylor et al., 2009; Takeuchi and Larson, 2005). Often, modern precipitation or surface water isotope-elevation relationships are used to estimate surface elevation and/or climate changes on the leeward side of mountain ranges where factors other than elevation have a significant impact (Cyr et al., 2005; Fan et al., 2014; Polissar et al., 2009). In many continental environments, evaporation of surface water and raindrops as they fall through the air significantly affects the isotopic composition of both precipitation and surface water, complicating the interpretation of stable isotope variations (Gat and Airey, 2006; Stewart, 1975; Yamada and Uyeda, 2006; Yang et al., 2007). In addition, surface water recycling, where continental surface water is evaporated and integrated into downwind precipitation, may result in isotopic patterns that deviate from simple temperature (elevation) dependent Rayleigh distillation models (Bershaw et al., 2012; Froehlich et al., 2008; Kurita and Yamada, 2008). Elsewhere, moisture source mixing has been inferred to cause both seasonal and spatial variability in the isotopic composition of meteoric water (Sjostrom and Welker, 2009; Tian et al., 2007), along with spatiotemporal variation in air trajectories (Lechler and Galewsky, 2013).

Isotopes of modern meteoric water have been used to constrain the spatial extent, magnitude, and temporal variability of the South American monsoon (Vuille et al., 2012; Vuille and Werner, 2005). Though variation in monsoon strength has been related to the height and/or extent of the Andes (Insel et al., 2009; Poulsen et al., 2010), the modeled effects of changing topography on precipitation patterns vary across the orogen (Garreaud et al., 2010; Jeffery et al., 2012). A better understanding of the forcing mechanisms behind modern changes in water chemistry across the Andean Plateau will enable us to better interpret proxy records of South American paleoelevation, paleoclimate, and by extension, predict future climate change. This is especially important considering an entire Andean civilization perished during an abrupt period of climate change to more arid conditions as recent as ~1100 AD (Binford et al., 1997), with implications for modern farmers on the Andean Plateau, who depend on monsoon rains for their livelihood (García et al., 2007).

Here, we present an extensive surface water dataset from the northern Andean Plateau, providing much needed constraints on modern water isotope evolution across the plateau and a context for the interpretation of elevation and climate proxies from the rock record in this continental environment. This dataset also adds fidelity to our understanding of precipitation source on the relatively arid western Andean Plateau and Western Cordillera. Stable isotope data from surface waters across the Andean Plateau presented here show: (1) a progressive increase in $\delta^{18}O$ west of the Eastern Cordillera that we attribute to a larger fraction of recycled water in precipitation and/or increase in evaporation downwind due to aridity; (2) an inverse relationship between $\delta^{18}O$ and elevation for water that has not experienced significant evaporation across the entire Andean Plateau including its flanks; (3) a general increase in $\delta^{18}O$ on the plateau from north to south due to an increase in evaporation and/or decrease in the amount effect due to aridity; and, (4) stable isotope and seasonal precipitation patterns that suggest easterlies transport the vast majority of moisture that falls as precipitation across the Andean Plateau and Western Cordillera from Peru to northern Bolivia (−13° to −20° latitude), with the Pacific contributing a minor amount near the coast.

2. BACKGROUND

2.1. Climate on the Andean Plateau

The Andean Plateau extends from approximately 15°S to 23°S, occupying the South American countries of Peru, Bolivia, Chile, and NW Argentina (Fig. 1). The climate across the northern Andean Plateau, including the Altiplano basin, Western and Eastern cordilleras, is characterized by large-scale (synoptic) atmospheric circulation modified by surface topography. The plateau itself averages about 4000 m elevation and is bound by the Western and Eastern cordilleras, which can reach elevations over 6000 m (Fig. 1).

Precipitation falls primarily during the austral summer, brought in by equatorial easterlies that originate in the Atlantic and traverse the Amazon Basin (Garreaud and Vuille, 2003; Lenters and Cook, 1997). Easterly circulation is driven by trade winds that converge on the inter-tropical convergence zone (ITCZ) across northern South America. As a whole, this topographic barrier receives intense precipitation on the eastern flank of the Eastern Cordillera, with increasingly dry conditions westward (Bookhagen and Strecker, 2008) and southward (Fiorella et al., 2015a; Garreaud and Vuille, 2003) (Fig. 2). Precipitation on the Andean Plateau is primarily convective and typically occurs during afternoon thunderstorms (Garreaud and Vuille, 2003; Houston and Hartley, 2003; Samuels-Crow et al., 2014a; Vuille and Keimig, 2004). West of the plateau, the Atacama Desert receives negligible precipitation (Miller, 1976). Relatively dry westerlies have been shown to contribute significantly to atmospheric circulation on the Western Cordillera and Andean Plateau, particularly during austral winter. However, westerlies apparently contribute very little to annual precipitation budgets (Aravena et al., 1999; Fiorella et al., 2015a).

2.2. Stable isotopes across the Amazon Basin and Eastern Cordillera

The isotopic composition ($\delta^{18}O$ and δD) of meteoric water across the Eastern Cordillera can be traced back to the equatorial Atlantic Ocean (Bershaw et al., 2010; Fiorella et al., 2015a; Gonfiantini et al., 2001). Progressive rain-out of atmospheric moisture westward across the

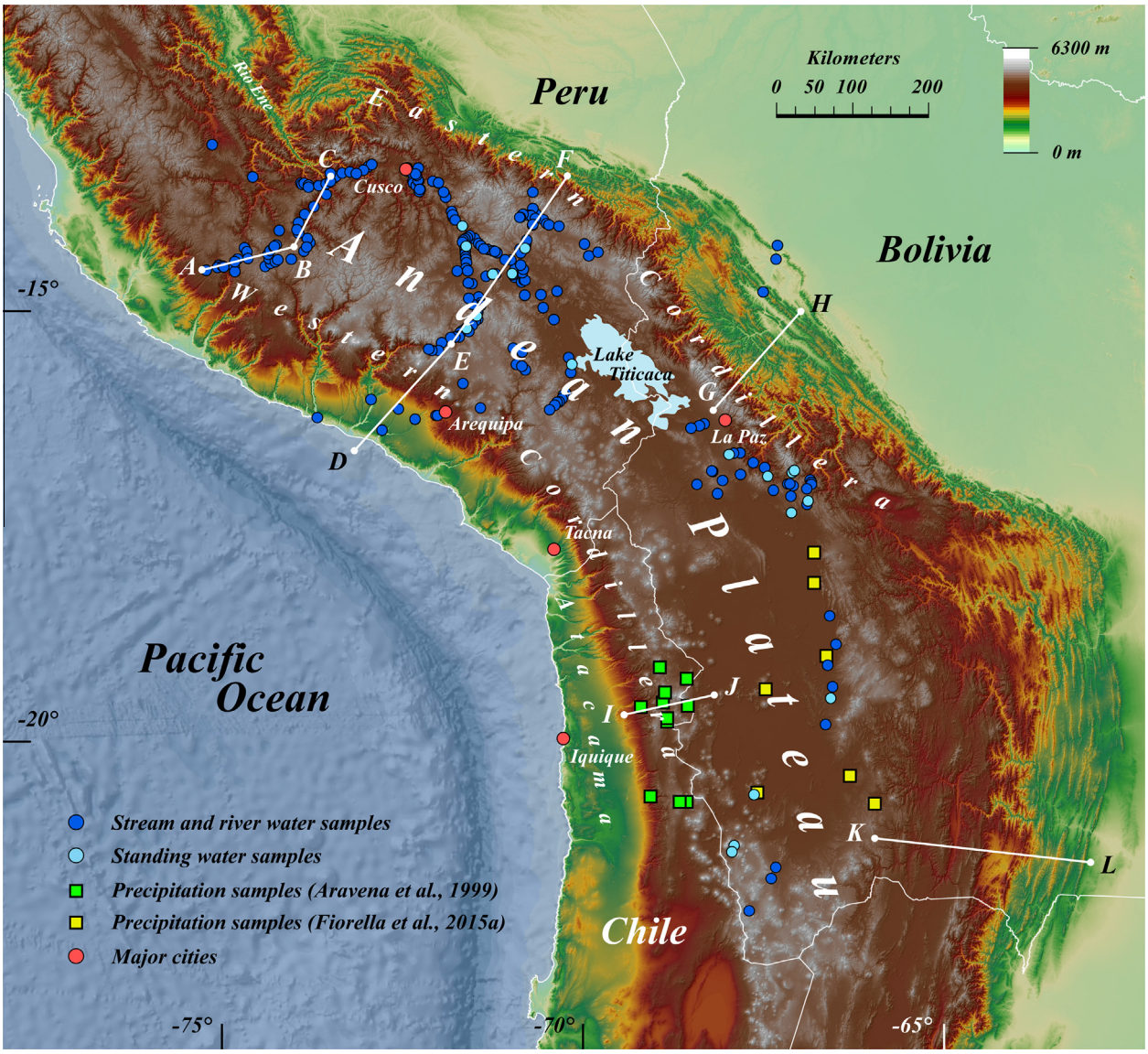

Fig. 1. Sample location map of surface water collected across the Andean Plateau and surrounding regions. Dark blue circles are surface stream and river water sample sites (Supplementary Table 1). Light blue circles are standing water sample sites (lakes, marshes, etc.) (Table 1). Green squares representing transect IJ are precipitation collection sites with data published by Aravena et al. (1999) (Table 2). Yellow squares are precipitation collection sites on the plateau published by Fiorella et al. (2015a) (Table 3). Transect KL corresponds with precipitation data from the same study, down the eastern (windward) flank of the Eastern Cordillera. Transect GH also corresponds with published surface water data from the windward side of the Eastern Cordillera (Bershaw et al., 2010; Gonfiantini et al., 2001). Red circles show locations of major cities. The basemap was derived from satellite data (SRTM from http://earthexplorer.usgs.gov/).

Amazon Basin results in a steady depletion of relatively heavy isotopes (the continental effect). This is attenuated by widespread transpiration resulting in a continental gradient in isotopic composition that is less than that observed in other continental environments (0.75–1.5‰/1000 km inland compared to 2‰/1000 km for Europe) (Rozanski et al., 1993; Salati et al., 1979). The isotopic composition of precipitation and surface water have been shown to inversely correlate with elevation from the lowlands of Brazil up the eastern (windward) flank of the Eastern Cordillera (Bershaw et al., 2010; Fiorella et al., 2015a; Gonfiantini et al., 2001). This pattern is consistent with the progressive removal of relatively heavy isotopes during orographic ascent and condensation of atmospheric moisture, typical of the windward side of mountain ranges globally (Poage and Chamberlain, 2001). The relationship between the isotopic composition of stream water and elevation breaks down south of −24° latitude along the Eastern Cordillera where convective storms dominate, masking the depletion of heavy isotopes in precipitation as a function of elevation. This observation is based on trends in stream water datasets located at −22° ($R^2 = 0.68$), −24° ($R^2 = 0.43$), and −26° ($R^2 = 0.17$) (Rohrmann et al., 2014).

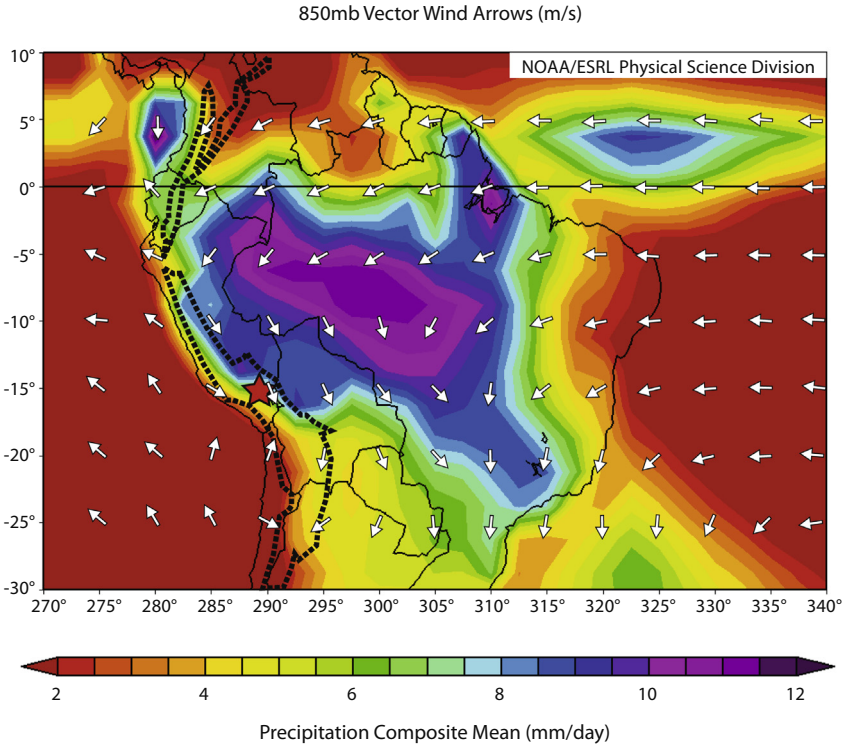

Fig. 2. Composite of NCEP/NCAR reanalysis data showing long-term average low-level (850 mb) wind vectors (white arrows) and Global Precipitation Climatology Project (GPCP) precipitation amount (colors) for South America during austral summer (DJF) from 1980 to 2015. Dashed black curve is a smoothed 4000 m elevation contour showing approximate outline of the Andes. Red star indicates region of sampling for this study. Image provided by the NOAA/ESRL Physical Sciences Division, Boulder Colorado from their Web site at http://www.esrl.noaa.gov/psd (Kalnay et al., 1996).

2.3. Stable isotopes on the Andean Plateau

Spatial patterns in water isotopes across the northern Andean Plateau, which sits on the leeward side of the Eastern Cordillera, are not well-constrained. However, Fiorella et al. (2015a) observe a significant correlation ($R^2 = 0.82$) between elevation and $\delta^{18}O$ of annual mean precipitation throughout the southern Altiplano and Eastern Cordillera (Fig. 1). Evaporation in an arid (low relative humidity) environment causes kinetic fractionation that often increases $\delta^{18}O$ values of residual surface water reservoirs (Gat, 1996; Stewart, 1975). Unlike precipitation, there is evidence that surface waters are highly evaporated across much of the southern Altiplano (Fiorella et al., 2015b). In addition, precipitation samples along transects up the Western Cordillera in northern Chile show a very steep isotopic lapse rate that is almost four times the global average, −10‰/km and −2.5‰/km, respectively (Aravena et al., 1999; Poage and Chamberlain, 2001). This has been interpreted by Aravena et al. (1999) to be the result of air mass mixing where Atlantic-derived moisture dominates precipitation at high elevations in the Western Cordillera and Pacific-derived moisture dominates at low elevations in the hyper-arid Atacama Desert.

To better understand controls on the isotopic composition of meteoric water for the Andean Plateau where evaporation may be significant, we report deuterium excess (*d excess* = $\delta D - 8^* \delta^{18}O$) values (Dansgaard, 1964; Stewart, 1975). A function of both H and O in a water sample, *d excess* may be used to constrain both the source of moisture and evaporative processes during and after transport in meteoric water samples (Froehlich et al., 2001). Relatively low *d excess* of precipitation is often associated with sub-cloud evaporation of raindrops during their descent through the air. Similarly, *d excess* can be lowered in surface water samples through evaporation, often seen in closed basin lakes with high residence times. Relatively high *d excess* values have been observed in moisture derived from the evaporation of surface water reservoirs (both marine and continental) at low relative humidity (Bershaw et al., 2012; Froehlich et al., 2008; Pang et al., 2011). Relatively high *d excess* values can also be caused by precipitation at very low temperatures, observed in Antarctica and at high elevation in some mountain ranges (Jouzel and Merlivat, 1984; Liotta et al., 2006; Samuels-Crow et al., 2014b).

3. METHODS

The strategy was to collect surface water samples, both with high and low residence time across the northern Andean Plateau to observe spatial patterns, including the magnitude of evaporation, across a region where little published data currently exists. We focused on sampling from

high elevation (>3500 m) on the plateau, but also collected lower elevation samples when convenient. We targeted rivers of all sizes and some standing water bodies. Because we are interested in using results to better understand long-term records, including those interpreted from paleowater proxies, we targeted rivers which average numerous precipitation events. Finding surface water to sample in the Western Cordillera was especially challenging considering the very arid climate there. In total, 275 water samples were collected throughout Peru and Bolivia from 2009 through 2014, during the months of May and June, from many sources.

Analyses completed at the University of Rochester were made by laser absorption spectroscopy on a Los Gatos Research Liquid Water Isotope Analyzer (LWIA-24d DLT-100) with a GC-PAL autosampler. Approximately 900 nl of water was injected into a heated, evacuated block. Water was vaporized and drawn into a laser cavity, where absorption analysis took place. Reported results are the average and standard deviation of 5–10 adjacent injections and measurements of a water sample from a single vial. Standardization is based on internal standards referenced to Vienna Standard Mean Ocean Water (VSMOW) and Vienna Standard Light Antarctic Precipitation (VSLAP). The 2σ uncertainties of H and O isotopic results are ±2.4‰ and ±0.20‰ respectively, unless otherwise indicated.

Analyses completed at the University of Arizona were made using a dual inlet mass spectrometer (Delta-S, Thermo Finnegan, Bremen, Germany) equipped with an automated chromium reduction device (H-Device, Thermo Finnegan) for the generation of H gas using metallic chromium at 750 °C. Water $\delta^{18}O$ was measured on the same mass spectrometer using an automated CO_2-H_2O equilibration unit. Standardization is also based on internal standards referenced to VSMOW and VSLAP. The 1σ uncertainties of H and O isotopic results from this lab are better than ±1‰ and ±0.08‰ respectively.

4. RESULTS

Results are listed in Supplementary Table 1 and Table 1 with $\delta^{18}O$ and *d excess* values mapped using natural neighbor interpolation in ArcGIS ArcMap version 10.3 in Figs. DR1A and DR1B respectively. Surface water isotopes from streams show significant variability across the Andean Plateau, from a minimum of −19.6‰ to a maximum of 5.6‰ (Supplementary Table 1). Standing water samples show similar variability with a range from −17.4‰ to 4.2‰ (Table 1). Because of the broad spatial variability in the dataset, we have produced a number of transects that highlight patterns observed in data subsets for the Eastern Cordillera (Fig. 3), across the Andean Plateau itself (Figs. 4–7), and in the Western Cordillera (Fig. 8). In each of the plots, elevation is measured as the mean basin hypsometry, which is the average elevation of the watershed upstream from the sample site. The centroid of stream catchments is used instead of sample location to better represent the geographic distribution of meteoric water contributing to the sample. Note that the locations shown in Fig. 1 are the sample sites, while locations shown in Figs. DR1A and DR1B are the centroid of associated watersheds.

5. DISCUSSION

5.1. Isotope trends up the Eastern Cordillera

On the windward flank of the Eastern Cordillera isotopic lapse rates are consistent with Rayleigh distillation of moisture during orographic ascent, as observed in global datasets (−2.8‰/km) (Poage and Chamberlain, 2001) and as predicted by thermodynamic modeling (Rowley, 2007; Rowley et al., 2001). West of Cusco, Peru, we observe an inverse relationship between $\delta^{18}O$ and elevation along transect BC up a tributary of the Rio Ene (Fig. 3), with an isotopic lapse rate of −2‰/km elevation gain. Samples included in this transect are noted in Supplementary Table 1. This is similar to the isotopic lapse rate of −1.9‰/km previously recorded up the windward (east) side of the Eastern Cordillera along transects GH and KL. (Bershaw et al., 2010; Fiorella et al., 2015a; Gonfiantini et al., 2001). This pattern reflects moisture transported from the Brazilian lowlands up through valleys in the Eastern Cordillera. Because watersheds that contribute to the Rio Ene (transect BC) penetrate deeply into the Andean Plateau from the north, we show that this $\delta^{18}O$-elevation relationship is seen over 100 km into the rainshadow of the Eastern Cordilleran crest. This suggests that water on the leeward (plateau) side of mountain ranges may still faithfully record paleoelevation as calibrated to the isotopic lapse rate on a range's windward flank where deep valleys provide pathways for moisture to bypass a mountain range's highest peaks.

5.2. Isotope trends on the Andean Plateau

5.2.1. Elevation

Systematic spatial patterns in the isotopic composition of meteoric water are notoriously challenging to discern on the leeward (rainshadow) side of mountain ranges (Bershaw et al., 2012; Hren et al., 2009; Lechler and Niemi, 2011a). Standing water was collected throughout the plateau with many samples showing extreme evaporation (negative *d excess*), typical of arid, closed basin environments (Table 1). Stream water also shows significant variability across the Andean Plateau, from a minimum of −19.6‰ to a maximum of 5.6‰ at elevations >3500 m, suggesting many streams are significantly affected by evaporative enrichment as well (Supplementary Table 1 and Fig. DR1). When the entire stream water dataset is considered, the vast majority of which is from the Andean Plateau itself, we do not observe a significant relationship between $\delta^{18}O$ and elevation ($R^2 = 0.12$) (Fig. 4A). Over half of stream water samples have *d excess* values <5‰ (Supplementary Table 1), suggesting that evaporative enrichment is creating considerable scatter in the data. Similar observations have been made in other relatively dry, continental regions including central Asia (Bershaw et al., 2012; Liu et al., 2015; Tian et al., 2007), in the southern Andean Plateau (Fiorella et al., 2015b;

Table 1
Catchment size, locality information, and stable isotope results for standing water (lakes, marshes, etc.) across the study area.

Sample ID	$\delta^{18}O$ (vsmow)	δD (vsmow)	d excess	Sample Site Elevation (m)	Mean Basin Hypsometry (m)	Latitude	Longitude	Latitude (Centroid)*	Longitude (Centroid)*	Catchment Size (km2)	Collection Date
10PE-26w	−14.4	−111	4.4	3495	4197	−14.196	−71.325	−14.324	−71.188	767	06-05-2010
10PE-33w	1.7	−23.1	−36.6	3927	4334	−14.765	−70.732	−14.581	−70.821	932	06-05-2010
10PE-47w	−2	−43.5	−27.8	3824	4170	−15.835	−70.014	−16.086	−69.545	83,038	08-05-2010
10PE-55w	−10.6	−97.1	−12.4	3966	4334	−14.437	−71.285	−14.523	−71.133	467	13-05-2010
10PE-79w	−14.9	−116.7	2.1	4219	4612	−15.403	−71.288	−15.523	−71.097	2,049	14-05-2010
B	−8.3	−66.6	−0.5	3838	3920	−17.154	−67.625	−17.183	−67.613	14	19-07-2007
Q	4.2	−12.7	−46.6	3856	3981	−17.578	−67.332	−17.552	−67.362	45	03-08-2007
R	−8.3	−52.7	13.5	4666	4671	−17.104	−67.324	−17.105	−67.323	1	04-08-2007
S	−6.5	−65.8	−14	4645	4730	−17.079	−67.301	−17.08	−67.299	0	04-08-2007
X	0.1	−30	−30.7	4225	4251	−16.898	−68.099	−16.895	−68.105	1	05-08-2007
IO	−4.9	−68	−28.8	3694	3876	−20.9	−67.764	−20.915	−67.725	393	27-05-2009
JO	−12.7	−96.2	5	4138	4623	−21.502	−68.008	−21.679	−67.999	858	28-05-2009
KO	−12	−92.4	3.5	4122	4674	−21.573	−68.039	−21.721	−67.974	626	28-05-2009
OO	−11	−109.8	−22.2	3864	4155	−19.754	−66.821	−19.858	−66.693	623	30-05-2009
Z10	3.6	−19.8	−48.5	4411	4463	−17.438	−67.129	−17.439	−67.129	3	16-08-2007
NPWS005	−9.9	−109.6	−30.4	4027	4145	−14.468	−70.576	−14.462	−70.584	15	22-05-2011
200511-03	−7.4	−111.5	−52.3	4789	4870	−15.258	−71.163	−15.257	−71.184	1	20-05-2011
280511-03	−17.4	−137.1	2.5	4530	4628	−14.767	−70.967	−14.764	−70.972	3	28-05-2011

* The centroid is defined as the geographic center of a catchment upstream from a sample site.

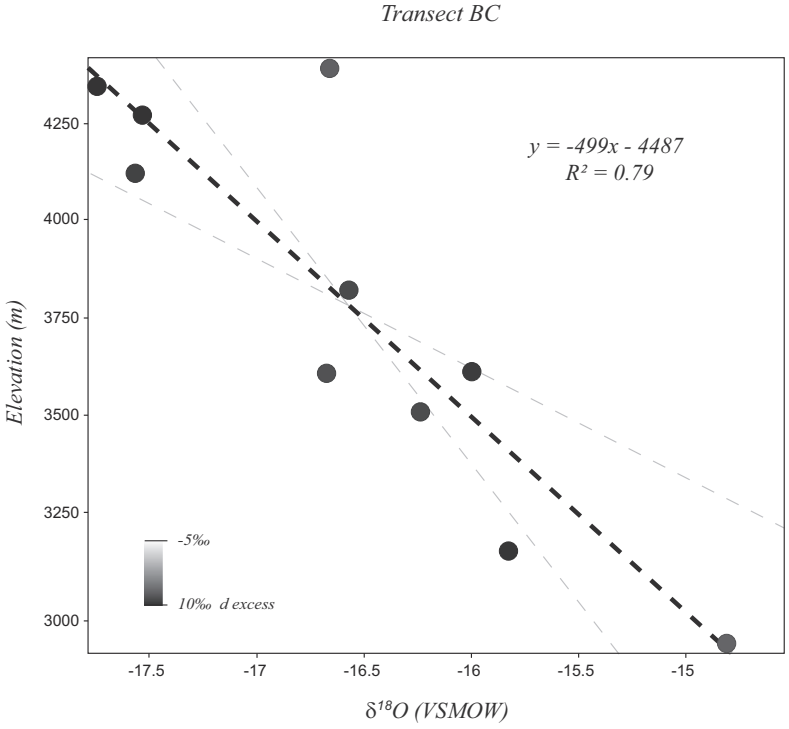

Fig. 3. A compilation of stream water data along an elevation transect on the plateau corresponding with transect BC in Fig. 1. The isotopic lapse rate is approximately −2‰/km elevation gain, consistent with transects up the windward side of the Eastern Cordillera. Circles are shaded by *d excess* value with a gradient from 10‰ (black) to −5‰ (white). 95% confidence intervals are shown as grey dashed lines. Elevation is reported as the mean basin hypsometry.

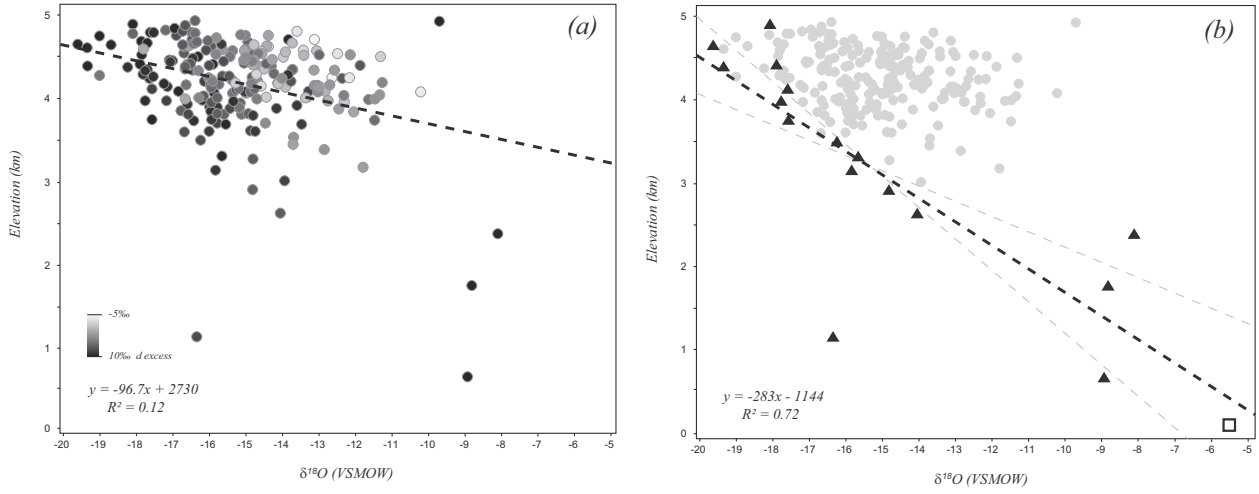

Fig. 4. (a) A compilation of $\delta^{18}O$ values (*x*-axis) for stream and river water samples collected from the Andean Plateau plotted against elevation (*y*-axis). A linear regression suggests there is not a significant relationship when the entire stream dataset is considered ($R^2 = 0.12$). (b) The most negative $\delta^{18}O$ values per 200 m elevation are denoted with triangles (noted in Supplementary Table 1 and Fig. DR1A). The open square shows the annual weighted mean of precipitation at Cuiaba and Manaus, Brazil (IAEA/WMO, 2016) at low elevation (<200 m) in the Andean foreland (NE of the map shown in Fig. 1). The black dashed line is a regression through these most negative $\delta^{18}O$ values (triangles and open square). 95% confidence intervals are shown as grey dashed lines. The standard error on this regression is 780 m. Lower elevation (<2.5 km) scatter may be due to low sample density. The isotopic lapse rate is ∼−3.5‰/1 km elevation gain, suggesting elevation exerts a first-order control on the isotopic composition of relatively non-evaporated surface water across the northern Andean Plateau. Symbols are shaded by *d excess* value with a gradient from 10‰ (black) to −5‰ (white). Elevation is reported as the mean basin hypsometry. Samples with extremely low *d excess* values <−5‰ (18 samples) are not included as they are likely affected significantly by evaporation.

Rohrmann et al., 2014), and the southwest United States (Lechler and Niemi, 2011b). However, we do observe an inverse relationship between $\delta^{18}O$ and elevation for the most negative $\delta^{18}O$ values (Fig. 4B). The sample subset used in this regression were chosen based on the most negative $\delta^{18}O$ value per 200 m elevation gain and are noted in Supplementary Table 1 and Fig. DR1 (triangles). The isotopic lapse rate for these most negative values collected across the entire plateau is -3.5‰/km ($R^2 = 0.72$). This indicates that the isotopic composition of water that has experienced minimal evaporation is controlled by changes in elevation across the entire Andean Plateau. The isotopic lapse rate across the plateau is steeper than that observed up the eastern (windward) side of the Eastern Cordillera (~−2‰/km) (Bershaw et al., 2010; Fiorella et al., 2015a; Gonfiantini et al., 2001). This may be due to evaporative enrichment at relatively low elevations and/or a larger contribution from low $\delta^{18}O$ snow at the highest elevations. These results are consistent with Fiorella et al. (2015a), who suggest that elevation is the most significant control on the isotopic composition of precipitation for the southern Altiplano ($R^2 = 0.82$). This relationship breaks down in stream water south of −24° latitude on the plateau's eastern flank where convective storms transport moisture vertically as opposed to orographic lifting, resulting in little to no isotopic lapse rate (Rohrmann et al., 2014).

5.2.2. Longitude

While the isotopic composition of surface waters across the Andean Plateau is apparently controlled by elevation, it is often heavily modified by surface water recycling and/or evaporative enrichment. Along transect DEF, which crosses the plateau in southern Peru (Fig. 1), we observe a general increase in the most positive $\delta^{18}O$ values of stream water southwestward while elevation remains relatively constant (Fig. 5). The isotopic composition of surface (stream) water also becomes more variable, with a range of ~3‰ in the northeast to ~6‰ in the southwest part of the plateau (maximum difference between samples 75 km and 225 km from the Andean foreland respectively). This trend is inconsistent with the continental effect, described from a global long-term precipitation dataset (Rozanski et al., 1993). The approximate rate of increase for the most positive values along this transect (~1‰/70 km) is conspicuously similar to that observed northward across the Tibetan Plateau (~1‰/72 km) (Bershaw et al., 2012; Hren et al., 2009; Li and Garzione, submitted for publication; Quade et al., 2011; Tian et al., 2001).

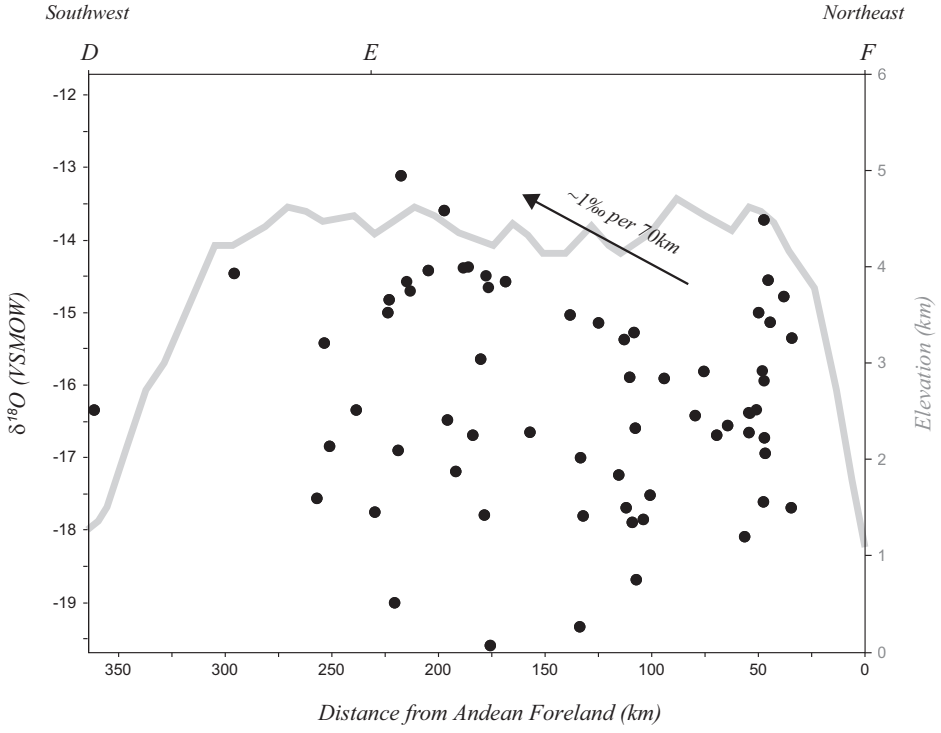

Fig. 5. A compilation of stream and river water samples along a NE–SW transect shown as DEF in Fig. 1. Only samples within 25 km of transect DEF are included (noted in Supplementary Table 1). The gray curve is the average elevation over a 100 km wide swath following this transect. $\delta^{18}O$ values of stream water decrease significantly up the windward side of the Eastern Cordillera. The most negative values (−19‰) correspond with an elevation of ~4.2 km based on the isotopic lapse rate in Fig. 4B. Westward across the plateau, the most positive values increase at a rate of ~1‰/70 km inland from the Eastern Cordilleran crest, consistent with recycling of evaporatively enriched surface waters. For sample locations, the geographic center of catchments upstream from stream or river sample sites (centroid) is used. Elevation is reported as the mean basin hypsometry. Three samples with very low *d excess* values <−5‰ are not included as they represent extreme evaporative enrichment (170511-01, 030611-01, and 10PE-88w).

The observation that the isotopic composition of meteoric water becomes progressively enriched at a similar rate deep into the rainshadow of both the Andean and Tibetan Plateaux suggests common processes during moisture transport, such as surface water recycling and/or evaporative enrichment, are responsible, as opposed to mixing of unique moisture sources, which would be unique to each region. On the Tibetan Plateau, surface water reservoirs are progressively enriched in ^{18}O through evaporation and partial removal (advection) of relatively low $\delta^{18}O$ vapor off the plateau. This trend is observed in *d excess* values which increase in streams but decrease in lakes downwind (north) from the Himalayan rainshadow (Bershaw et al., 2012). As the recycling ratio increases downwind (westward) across the Andean Plateau, the proportion of locally-derived moisture versus that advected from outside the plateau increases (Trenberth, 1999). Standing water, a source of recycled precipitation on the plateau, also shows evidence of evaporative enrichment (high in $\delta^{18}O$ and low in *d excess*) (Table 1). Continental recycling ratios in South America have been shown to reach a maximum near the Western Cordillera of ~70% (Van der Ent et al., 2010). Similar to the Tibetan Plateau, a larger contribution of recycled surface water to precipitation downwind may contribute to increasing $\delta^{18}O$ values of streams (Fig. 2). However, the relationship between stream water *d excess* and distance from the Andean foreland along transect DEF is weak to non-existent ($R^2 = 0.003$) (Fig. DR2).

It is also possible that stream water samples are enriched prior to sampling through surface water evaporation and/or subcloud evaporation of raindrops as they fall through the air (Gat and Airey, 2006). According to this model, we would expect a progressive increase in evaporation downwind to result in an inverse relationship between *d excess* and distance from the Andean foreland. Though this relationship is not clear in our stream water dataset, precipitation samples from Fiorella et al. (2015a) and Aravena et al. (1999) (Tables 2 and 3) on the southern plateau (elevation > 3500 m) do show an inverse relationship with distance from the Andean foreland (longitude) ($R^2 = 0.69$), suggesting evaporative enrichment due to subcloud evaporation plays a significant role (Fig. 6A). While precipitation *d excess* decreases downwind (westward) across the Andean Plateau, $\delta^{18}O$ values of precipitation do not exhibit an obvious trend, possibly due to the wide range in latitude and poor sample representation between −67° and −68.5° longitude (Fig. 6B). The observation that there is not a clear decrease in precipitation $\delta^{18}O$ values to the west is consistent with evaporative enrichment mitigating the continental effect.

5.2.3. Latitude

Because this dataset does not include many locations south of −18°, published precipitation datasets from Aravena et al. (1999) and Fiorella et al. (2015a) have been included in a plot of latitudinal variation (Fig. 7). When

Table 2
Locality information and stable isotope results for precipitation samples published by Aravena et al. (1999).

Sample location	$\delta^{18}O$ (vsmow)*	δD (vsmow)*	d excess	Sample Site Elevation (m)	Latitude	Longitude	Precipitation Amount (mm)
POROMA	−4.5	−21.4	14.3	2880	−19.867	−69.183	41
HUATACONDO	−11.4	−79.9	11.5	2460	−20.917	−69.05	15
PUCHULDIZA	−14.4	−104	11.2	4200	−19.4	−68.95	100
COLCHANE	−14.9	−106.3	13.3	4100	−19.7	−68.883	208
HUAYTANE	−14.1	−100.9	11.9	3790	−19.543	−68.604	161
CANCOSA	−14	−96.4	15.6	3850	−19.85	−68.6	143
PAMPA LIRIMA	−9.8	−67.8	10.9	4100	−19.82	−68.9	79
PARCA	−6.6	−40.9	12.2	2700	−20.017	−68.85	20
COLLACAGUA	−10.2	−68.6	12.8	3960	−20.033	−68.85	147
COLLAGUASI	−22.1	−165.9	11.1	4550	−20.983	−68.7	43
UJINA	−10	−68.4	11.6	4200	−20.983	−68.6	123

* Stable isotope averages are weighted by precipitation amount for each site.

Table 3
Locality information and stable isotope results for precipitation samples published by Fiorella et al. (2015a).

Sample Location	$\delta^{18}O$ (vsmow)	δD (vsmow)	d excess	Sample Site Elevation (m)	Latitude	Longitude	Precipitation Amount (mm)*
SAN JUAN	−14.3	−99.8	14.6	3663	−20.9	−67.76	162
SALINAS	−17.5	−122.6	17.4	3719	−19.65	−67.64	255
NOEL MARIACA	−14.1	−97.8	15	3780	−20.68	−66.64	169
GRAN CHOCAYA	−14	−92	20	4340	−20.97	−66.33	227
ORURO	−15.5	−107.1	16.9	3718	−17.98	−67.11	401
EL CHORO	−15.6	−109.2	15.6	3706	−18.36	−67.11	547
QUILLACAS	−15.5	−108.1	15.9	3780	−19.23	−66.94	360

* Average per year for 3–5 years.

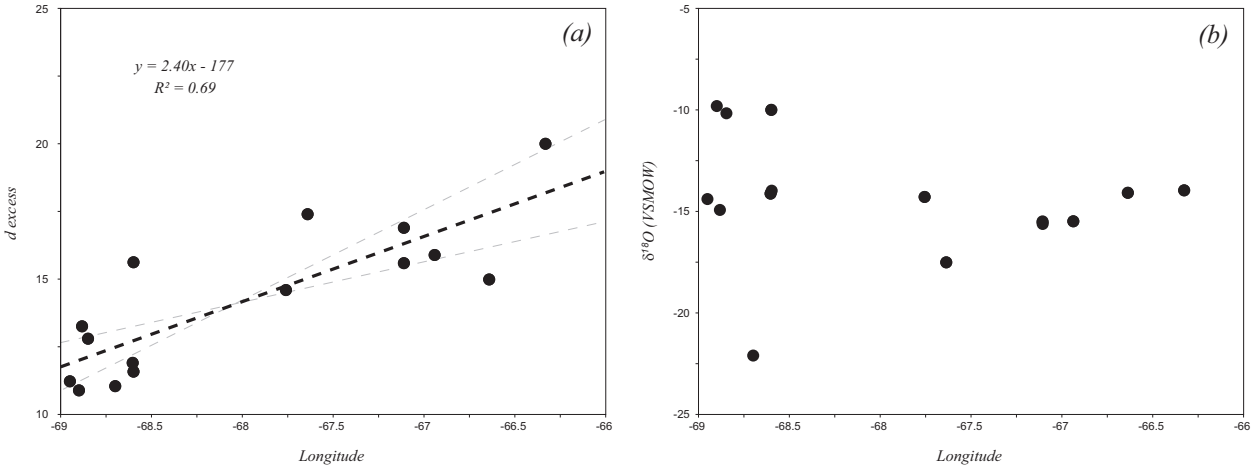

Fig. 6. (a) A compilation of published precipitation data from Aravena et al. (1999) (Table 2) and Fiorella et al. (2015a) (Table 3). Sample locations are throughout the central and southern Andean Plateau (Fig. 1). *d excess* values are plotted against longitude as this part of the Andean Plateau strikes roughly north–south. Though we do not see a meaningful trend in *d excess* from stream water samples (Fig. DR2), *d excess* in precipitation decreases with distance from the Andean foreland, suggesting evaporative enrichment through subcloud evaporation becomes increasingly significant westward (downwind). (b) Interestingly, there is not a meaningful trend in $\delta^{18}O$ values of precipitation in the same dataset. The observation that there is not a clear decrease in precipitation $\delta^{18}O$ values to the west may be interpreted as evaporative enrichment mitigating the continental effect downwind.

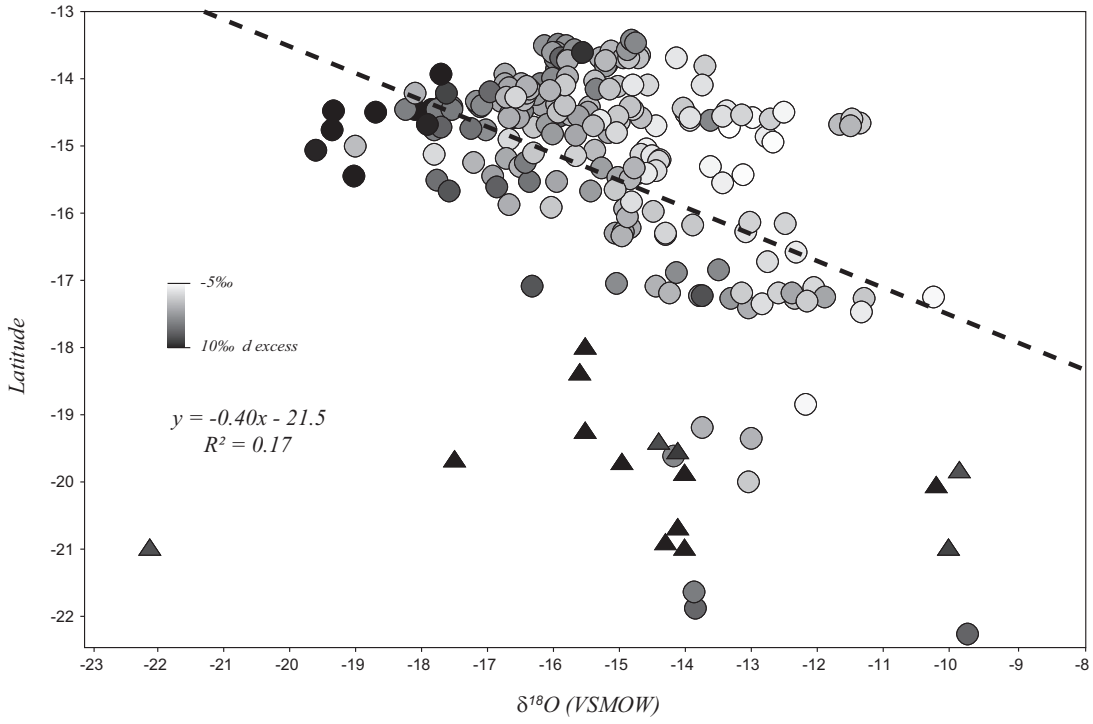

Fig. 7. A compilation of $\delta^{18}O$ values (*x*-axis) for stream (circles) and precipitation (triangles) samples from the Andean Plateau plotted against latitude (*y*-axis). Stream data (circles) are from this study (Supplementary Table 1) while precipitation data (triangles) are from Aravena et al. (1999) (Table 2) and Fiorella et al. (2015a) (Table 3). Published precipitation data was added south of −18° due to a paucity of stream data there. Symbols are shaded by *d excess* value with a gradient from 10‰ (black) to −5‰ (white). The black dashed line is a regression through this combined dataset showing a weak correlation ($R^2 = 0.17$). Though there is considerable scatter, it appears that $\delta^{18}O$ values are generally more positive on the southern Andean plateau, consistent with more arid conditions there. For stream samples, the geographic center of catchments upstream from stream or river sample sites (centroid) is used and elevation is reported as the mean basin hypsometry. Only samples from elevations >3500 m are included, limiting the dataset to the plateau itself. Samples with extremely low *d excess* values <−5‰ (15 samples) are not included as they are likely significantly affected by evaporation.

considering these combined datasets, the correlation between isotopic composition and latitude is weak ($R^2 = 0.17$). That said, it appears there is a general shift towards more positive values on the southern Andean Plateau, even in samples with consistently high (>10‰) *d excess* values. A latitudinal gradient in isotopic composition, where $\delta^{18}O$ values are more positive in the south, would be contrary to global patterns where $\delta^{18}O$ values of meteoric water are observed to decrease at higher latitudes (e.g. Rozanski et al., 1993). On the Andean Plateau, the south receives less precipitation than the north. Modern rainfall estimates range from >50 cm/yr north of 18°S to <25 cm/yr south of 20°S (Bookhagen and Strecker, 2008; Garreaud and Vuille, 2003; IAEA/WMO, 2016). Higher precipitation amounts in the north are also influenced by Lake Titicaca, a likely source of recycled moisture (García et al., 2007). Higher $\delta^{18}O$ of surface water in the southern Andean Plateau may be due to this climate gradient leading to higher rates of evaporation (Gat and Airey, 2006) and/or decreased amount effect precipitation and convective moistening on the southern Andean Plateau (Galewsky and Samuels-Crow, 2015). Surface water reservoirs often exhibit high $\delta^{18}O$ and very low *d excess* (Table 1) suggesting evaporation post-deposition is significant. If surface water and/or subcloud evaporation were more intense in the south, one might predict that *d excess* values would be more negative. However, similar to observations made on the Andean Plateau's southeast flank, we do not observe systematic changes in *d excess* with latitude (Rohrmann et al., 2014). Relatively dry conditions in the south may also decrease the amount of convective moistening (amount effect) there, resulting in relatively high $\delta^{18}O$ values of meteoric water.

5.3. Isotope trends up the Western Cordillera

There is a unique relationship between $\delta^{18}O$ and elevation along transects AB and DE, up the western flank of the Western Cordillera in Peru (Fig. 1). These stream water data show a consistently steep isotopic lapse rate of −10‰/km elevation gain (Fig. 8). A remarkably similar pattern was observed in precipitation data farther south along transect IJ by Aravena et al. (1999). An isotopic lapse rate of this magnitude is not consistent with Rayleigh distillation of westerly-derived moisture from the Pacific Ocean (Rowley, 2007). It contrasts with isotopic lapse rates observed up the windward side of the Eastern Cordillera (∼−2‰/km) presented here along transect BC (Fig. 3) and along transects GH and KL in Fig. 1 (Bershaw et al., 2010; Fiorella et al., 2015a; Gonfiantini et al., 2001), consistent with easterly (Atlantic) derived precipitation. These anomalously steep isotopic lapse rates up the flank of the Western Cordillera likely represent mixing between highly evolved Atlantic moisture (low $\delta^{18}O$ values) and Pacific-derived fog and/or drizzle at low elevations (high $\delta^{18}O$ values). The Western Cordillera appears to be a transition zone, where the relative influence of easterly (Atlantic) derived moisture increases with elevation. Climate modeling corroborates this interpretation as easterlies contribute more to atmospheric circulation in the Western Cordillera during precipitation events (Aravena et al., 1999; Fiorella et al., 2015a; Garreaud et al., 2009).

Additional evidence is found in seasonal patterns of precipitation for sites throughout the region. La Paz, Bolivia receives most of its precipitation during austral summer (Dec, Jan, Feb, and Mar) (Figs. 1 and DR3). Precipitation that falls in La Paz is ultimately Atlantic-derived moisture that crosses the Amazon Basin before climbing up valleys that dissect the Eastern Cordillera, recycled many times along the way (Gonfiantini et al., 2001). Though Arequipa, Peru is located much farther downwind, across the plateau in the Western Cordillera, it displays a very similar seasonal pattern of precipitation with the vast majority also falling during austral summer. Closer to the Pacific Ocean, both Tacna, Peru and Iquique, Chile are the opposite, receiving precipitation primarily during austral winter (Jun, Jul, Aug), with dramatically less annual precipitation. These observations suggest that easterlies dominate at high and mid-elevations in the Western Cordillera, but do not contribute significantly to precipitation at low elevations near the Pacific coast. This may explain an anomalously steep isotopic lapse rate as relatively low $\delta^{18}O$ (depleted), Atlantic-derived moisture in the Western Cordillera transitions to relatively high $\delta^{18}O$ (enriched), Pacific-derived fog and/or drizzle at low elevations in Peru and Chile.

Intense evaporation of surface waters at low elevations near the Pacific coast may also contribute to the steep isotopic lapse rate as the total amount of annual precipitation decreases by orders of magnitude down the Western Cordilleran flank (Fig. DR3). This is seen in *d excess* values of streams which are relatively negative at low elevations near the Pacific Ocean, consistent with evaporative enrichment. Because precipitation samples from Aravena et al. (1999) do not show relatively low *d excess* values near the coast, it can be inferred that stream samples are primarily experiencing evaporation post-deposition (Figs. 8 and DR1B).

5.4. Studies of Paleoclimate and Paleoaltimetry

The isotopic composition of paleowater from the Andean Plateau is often estimated using proxies from the rock record (Garzione et al., 2008; Kar et al., 2016; Leier et al., 2013; Saylor and Horton, 2014). Though some may exhibit seasonal bias (Breecker et al., 2009), isotopic proxies have the benefit of time-averaging, reflecting paleoclimate. Across the Andean Plateau, surface water evaporation, evaporation of raindrops as they fall through the air, surface water recycling, and air mass mixing affect the isotopic composition of surface waters to varying degrees. To minimize the effect of post-depositional evaporation, proxies that integrate water with a short residence time at the surface should be targeted. Sedimentary carbonates, volcanic glass, lipid biomarkers, fossil teeth, and hydrated clays occur in diverse depositional environments and have all been used as proxies for the isotopic composition of paleowater (Bershaw et al., 2010; Canavan et al., 2014; Garzione et al., 2008; Mulch et al., 2006; Polissar et al., 2009; Saylor and Horton, 2014). The likelihood of evaporative enrichment depends partly on the depositional environment. Lacustrine and/or fluvial proxies may be

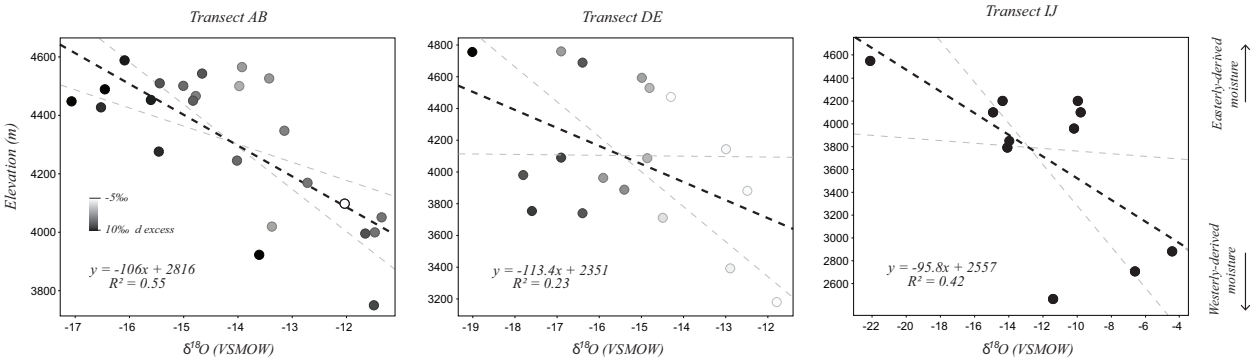

Fig. 8. Compilations of stream water data along three elevation transects on the western flank of the Andean Plateau (Fig. 1). The black dashed lines are linear regressions through the datasets. 95% confidence intervals are shown as grey dashed lines. The isotopic lapse rate of all three transects is consistently ~−10‰/km elevation gain. This steep isotopic lapse rate is likely due to air mass mixing and/or evaporation at low elevations near the coast. Samples included in each transect are noted in Supplementary Table 1. Unlike Fig. 3, samples more than 25 km from transect DE are included as sample density in this area is low. One anomalous low elevation site is excluded from transect DE (sample 20140518-04). The watershed of this sample is likely not defined correctly as its $\delta^{18}O$ value is consistent with other high elevation sites. Transect IJ shows weighted mean precipitation data from Aravena et al. (1999) (Table 2). Significant scatter (low R^2 value) is consistent with the effects of evaporation in arid environments. Circles are shaded by *d excess* value with a gradient from 10‰ (black) to −5‰ (white). Samples with extremely low *d excess* values <−5‰ are not included as they are likely significantly affected by evaporation. Elevation is reported as the mean basin hypsometry.

evaporatively enriched if surface water is exposed to the atmosphere, particularly if relative humidity is low and residence times are high. For this reason, paleosol proxies may be less susceptible to evaporative enrichment. However, the isotopic composition of soil water may also become enriched in arid environments, particularly if samples are from <50 cm depth (Cerling and Quade, 1993; Quade et al., 2011, 2007).

The likelihood of evaporation in arid environments means that large datasets should be obtained to effectively distinguish between samples that have and have not been evaporatively enriched. Considering the wide range of $\delta^{18}O$ values observed across the Andean Plateau, individual samples are not a good predictor of elevation (Fig. 4A). In some cases, evaporatively enriched samples (e.g. 170511-01) collected at over 3500 m elevation predict elevations at sea-level using the isotopic lapse rate from Fig. 4B. Proxies that reflect highly evaporated paleowater have similar potential to significantly underestimate paleoelevation.

Of 242 stream water samples, we took the most negative $\delta^{18}O$ value per 200 m elevation to establish an isotopic lapse rate (−3.5‰/km) across the plateau. Stream water samples that plot within 780 m of the trend line (standard error) are within statistical uncertainty of the regression. For the plateau (elevations > 3500 m), where evaporative enrichment of meteoric water can be pronounced, 26% of stream samples fall within the standard error, suggesting that a quarter of all samples are useful for predicting elevation. This highlights the importance of using the most negative of numerous samples to constrain paleoelevation in relatively arid environments such as the Andean Plateau. This does not account for additional proxy considerations, each of which have unique uncertainties associated with their recording of paleowater chemistry (Rowley and Garzione, 2007).

Using the modern isotopic lapse rate established up the Eastern Cordillera (−2‰/km) for paleowater proxies in the Eastern Cordillera is warranted. However, using the same isotopic lapse rate for sites in the western Altiplano and Western Cordillera is likely to result in underestimates of paleoelevation and overestimates of temperature. That said, this data shows that the most negative isotopic values still exhibit a significant relationship with elevation (Fig. 4B), suggesting that given a large enough sample population, paleoelevation constraints based on the most negative values and an appropriate isotopic lapse rate are justified, even deep into the rainshadow of a mountain range.

6. CONCLUSIONS

The northern Andean Plateau shows patterns of stable isotope evolution that appear dominated by processes that fractionate during and after vapor transport from the Atlantic via the Amazon Basin, with mixing between easterly and westerly (Pacific) derived moisture limited to the western flank of the Western Cordillera. Considerable recycling and/or evaporative enrichment of meteoric water across the Andean Plateau will likely lead to underestimates of paleoelevation, unless a sufficient number of samples are obtained to distinguish minimally evaporated samples. The most negative $\delta^{18}O$ values of stream water across the entire Andean Plateau show a significant relationship with elevation (−3.5‰/km) that is unique to this arid environment, and different from that observed on the relatively wet, windward flank of the Eastern Cordillera (−2‰/km). Therefore, we recommend using this steeper isotopic lapse rate for proxies obtained from the Andean Plateau itself.

Spatial patterns of isotope variability due to moisture source mixing appear limited to the coastal flank of the Western Cordillera, where we interpret a transition from Atlantic-derived moisture at high elevations to Pacific-derived fog and/or drizzle at lower elevations. This is supported by consistently steep isotopic lapse rates

(−10‰/km) along the Western Cordillera from Peru to Chile (Fig. 8), climate modeling (Aravena et al., 1999), and seasonal patterns of precipitation (Fig. DR3). We conclude that elevation exhibits a primary control on the isotopic composition of surface waters across the Andean Plateau and its flanks (−13° to −20° latitude), often modified significantly by surface water recycling and/or evaporation.

ACKNOWLEDGEMENTS

Thank you to Penny Higgins for help in running samples at SIREAL (University of Rochester) and to Katherine DeLoach for assistance in calculating watersheds for samples. Also, to Robinson Cecil and Nicholas Perez for help collecting samples in the field and Ken Cruikshank for statistical advice. Lastly, thank you to two anonymous reviewers whose feedback greatly improved this manuscript. This work was partially funded by NSF EAR-0908858 and EAR-1338694 to Garzione.

APPENDIX A. SUPPLEMENTARY DATA

Supplementary data associated with this article can be found, in the online version, at http://dx.doi.org/10.1016/j.gca.2016.08.011.

REFERENCES

Aravena R., Suzuki O., Pena H., Pollastri A., Fuenzalida H. and Grilli A. (1999) Isotopic composition and origin of the precipitation in Northern Chile. *Appl. Geochem.* **14**, 411–422.

Bershaw J., Garzione C. N., Higgins P., MacFadden B. J., Anaya F. and Alvarenga H. (2010) Spatial-temporal changes in Andean plateau climate and elevation from stable isotopes of mammal teeth. *Earth Planet. Sci. Lett.* **289**, 530–538.

Bershaw J., Penny S. M. and Garzione C. N. (2012) Stable isotopes of modern water across the Himalaya and eastern Tibetan Plateau: implications for estimates of paleoelevation and paleoclimate. *J. Geophys. Res. Atmos.* **1984–2012**, 117.

Binford M. W., Kolata A. L., Brenner M., Janusek J. W., Seddon M. T., Abbott M. and Curtis J. H. (1997) Climate variation and the rise and fall of an Andean civilization. *Quatern. Res.* **47**, 235–248.

Bookhagen B. and Strecker M. R. (2008) Orographic barriers, high-resolution TRMM rainfall, and relief variations along the eastern Andes. *Geophys. Res. Lett.* **35**.

Breecker D., Sharp Z. and McFadden L. (2009) Seasonal bias in the formation and stable isotopic composition of pedogenic carbonate in modern soils from central New Mexico, USA. *Geol. Soc. Am. Bull.* **121**, 630.

Canavan R. R., Carrapa B., Clementz M. T., Quade J., DeCelles P. G. and Schoenbohm L. M. (2014) Early Cenozoic uplift of the Puna Plateau, Central Andes, based on stable isotope paleoaltimetry of hydrated volcanic glass. *Geology* **42**, 447–450.

Cerling T. E. and Quade J. (1993) Stable carbon and oxygen isotopes in soil carbonates. *Clim. Change Cont. Isot. Rec.* **78**, 217–231.

Currie B. S., Polissar P. J., Rowley D. B., Ingalls M., Li S., Olack G. and Freeman K. H. (2016) Multiproxy paleoaltimetry of the Late Oligocene-Pliocene Oiyug Basin, southern Tibet. *Am. J. Sci.* **316**(5), 401–436.

Cyr A. J., Currie B. S. and Rowley D. B. (2005) Geochemical evaluation of Fenghuoshan Group lacustrine carbonates, north-central Tibet: implications for the paleoaltimetry of the Eocene Tibetan Plateau. *J. Geol.* **113**, 517–533.

Dansgaard W. (1964) Stable isotopes in precipitation. *Tellus* **16**, 436–468.

Fan M., Heller P., Allen S. D. and Hough B. G. (2014) Middle Cenozoic uplift and concomitant drying in the central Rocky Mountains and adjacent Great Plains. *Geology* **42**, 547–550.

Fiorella R. P., Poulsen C. J., Pillco Zolá R. S., Barnes J. B., Tabor C. R. and Ehlers T. A. (2015a) Spatiotemporal variability of modern precipitation δ18O in the central Andes and implications for paleoclimate and paleoaltimetry estimates. *J. Geophys. Res. Atmos.*.

Fiorella R. P., Poulsen C. J., Zolá R. S. P., Jeffery M. L. and Ehlers T. A. (2015b) Modern and long-term evaporation of central Andes surface waters suggests paleo archives underestimate Neogene elevations. *Earth Planet. Sci. Lett.* **432**, 59–72.

Froehlich, K., Gibson, J. and Aggarwal, P. (2001) Deuterium excess in precipitation and its climatological significance, Study of Environmental Change Using Isotope Techniques. Proc. Intern. Conf. Citeseer, pp. 54–66.

Froehlich K., Kralik M., Papesch W., Rank D., Scheifinger H. and Stichler W. (2008) Deuterium excess in precipitation of Alpine regions–moisture recycling. *Isot. Environ. Health Stud.* **44**, 61–70.

Galewsky J. and Samuels-Crow K. (2015) Summertime moisture transport to the southern south American Altiplano: constraints from in situ measurements of water vapor isotopic composition. *J. Clim.* **28**, 2635–2649.

García M., Raes D., Jacobsen S.-E. and Michel T. (2007) Agroclimatic constraints for rainfed agriculture in the Bolivian Altiplano. *J. Arid Environ.* **71**, 109–121.

Garreaud R., Vuille M., Compagnucci R. and Marengo J. (2009) Present-day South American climate. *Palaeogeogr. Palaeoclimatol. Palaeoecol.* **281**, 180–195.

Garreaud R. and Vuille M. C. A. C. (2003) The climate of the Altiplano; observed current conditions and mechanisms of past changes. In *Paleoclimates of the Central Andes* (eds. G. O. Seltzer, D. T. Rodbell and H. E. Wright). Elsevier, pp. 5–22.

Garreaud R. D., Molina A. and Farias M. (2010) Andean uplift, ocean cooling and Atacama hyperaridity: a climate modeling perspective. *Earth Planet. Sci. Lett.* **292**, 39–50.

Garzione C. N., Quade J., DeCelles P. G. and English N. B. (2000) Predicting paleoelevation of Tibet and the Himalaya from $\delta^{18}O$ vs. altitude gradients of meteoric water across the Nepal Himalaya. *Earth Planet. Sci. Lett.* **183**, 215–229.

Garzione C. N., Hoke G. D., Libarkin J. C., Withers S., MacFadden B., Eiler J., Ghosh P. and Mulch A. (2008) Rise of the Andes. *Science* **320**, 1304.

Gat J. (1996) Oxygen and hydrogen isotopes in the hydrologic cycle. *Annu. Rev. Earth Planet. Sci.* **24**, 225–262.

Gat J. R. and Airey P. L. (2006) Stable water isotopes in the atmosphere/biosphere/lithosphere interface: scaling-up from the local to continental scale, under humid and dry conditions. *Global Planet. Change* **51**, 25–33.

Gonfiantini R., Roche M.-A., Olivry J.-C., Fontes J.-C. and Zuppi G. M. (2001) The altitude effect on the isotopic composition of tropical rains. *Chem. Geol.* **181**, 147–167.

Houston J. and Hartley A. J. (2003) The central Andean west-slope rainshadow and its potential contribution to the origin of hyper-aridity in the Atacama Desert. *Int. J. Climatol.* **23**, 1453–1464.

Hren M. T., Bookhagen B., Blisniuk P. M., Booth A. L. and Chamberlain C. P. (2009) Δ 18 O and δD of streamwaters across the Himalaya and Tibetan Plateau: implications for moisture sources and paleoelevation reconstructions. *Earth Planet. Sci. Lett.* **288**, 20–32.

IAEA/WMO (2016) Global Network of Isotopes in Precipitation. The GNIP Database. Accessible at: http://isohis.iaea.org, The GNIP Database. Accessible at: http://isohis.iaea.org.

Insel N., Poulsen C. and Ehlers T. (2009) Influence of the Andes Mountains on South American moisture transport, convection, and precipitation. *Clim. Dyn.*, 1–16.

Jeffery M. L., Poulsen C. J. and Ehlers T. A. (2012) Impacts of Cenozoic global cooling, surface uplift, and an inland seaway on South American paleoclimate and precipitation δ18O. *Geol. Soc. Am. Bull.* **124**, 335–351.

Jouzel J. and Merlivat L. (1984) Deuterium and oxygen 18 in precipitation: Modeling of the isotopic effects during snow formation. *J. Geophys. Res. Atmos.* **89**, 11749–11757.

Kalnay E., Kanamitsu M., Kistler R., Collins W., Deaven D., Gandin L., Iredell M., Saha S., White G. and Woollen J. (1996) The NCEP/NCAR 40-year reanalysis project. *Bull. Am. Meteorol. Soc.* **77**, 437–471.

Kar N., Garzione C. N., Jaramillo C., Shanahan T., Carlotto V., Pullen A., Moreno F., Anderson V., Moreno E. and Eiler J. (2016) Rapid regional surface uplift of the northern Altiplano plateau revealed by multiproxy paleoclimate reconstruction. *Earth Planet. Sci. Lett.* **447**, 33–47.

Kent-Corson M., Ritts B., Zhuang G., Bovet P., Graham S. and Page Chamberlain C. (2009) Stable isotopic constraints on the tectonic, topographic, and climatic evolution of the northern margin of the Tibetan Plateau. *Earth Planet. Sci. Lett.* **282**, 158–166.

Kurita N. and Yamada H. (2008) The role of local moisture recycling evaluated using stable isotope data from over the middle of the Tibetan Plateau during the monsoon season. *J. Hydrometeorol.* **9**, 760–775.

Lechler A. R. and Galewsky J. (2013) Refining paleoaltimetry reconstructions of the Sierra Nevada, California, using air parcel trajectories. *Geology* **41**, 259–262.

Lechler A. R. and Niemi N. A. (2011a) Controls on the spatial variability of modern meteoric δ18O: empirical constraints from the western US and East Asia and implications for stable isotope studies. *Am. J. Sci.* **311**, 664–700.

Lechler A. R. and Niemi N. A. (2011b) The influence of snow sublimation on the isotopic composition of spring and surface waters in the southwestern United States: Implications for stable isotope–based paleoaltimetry and hydrologic studies. *Geol. Soc. Am. Bull.* **B30467**, 30461.

Leier A., McQuarrie N., Garzione C. and Eiler J. (2013) Stable isotope evidence for multiple pulses of rapid surface uplift in the Central Andes, Bolivia. *Earth Planet. Sci. Lett.* **371**, 49–58.

Lenters J. and Cook K. (1997) On the origin of the Bolivian high and related circulation features of the South American climate. *J. Atmos. Sci.* **54**, 656–678.

Li L. and Garzione C.N. (submitted for publication) Spatial distribution and controlling factors of stable isotopes in meteoric waters on the Tibetan Plateau: implications for paleoelevation reconstructions. Earth Planet. Sci. Lett.

Liotta M., Favara R. and Valenza M. (2006) Isotopic composition of the precipitations in the central Mediterranean: origin marks and orographic precipitation effects. *J. Geophys. Res. Atmos.* **1984–2012**, 111.

Liu Q., Tian L., Wang J., Wen R., Weng Y., Shen Y., Vladislav M. and Kanaev E. (2015) A study of longitudinal and altitudinal variations in surface water stable isotopes in West Pamir, Tajikistan. *Atmos. Res.* **153**, 10–18.

Miller A. (1976) The climate of Chile. *World Surv. Climatol.* **12**, 113–145.

Mulch A. (2016) Stable isotope paleoaltimetry and the evolution of landscapes and life. *Earth Planet. Sci. Lett.* **433**, 180–191.

Mulch A., Graham S. A. and Chamberlain C. P. (2006) Hydrogen isotopes in Eocene river gravels and paleoelevation of the Sierra Nevada. *Science* **313**, 87–89.

Pang Z., Kong Y., Froehlich K., Huang T., Yuan L., Li Z. and Wang F. (2011) Processes affecting isotopes in precipitation of an arid region. *Tellus B* **63**, 352–359.

Poage M. A. and Chamberlain C. P. (2001) Empirical relationships between elevation and the stable isotope composition of precipitation and surface waters; considerations for studies of paleoelevation change. *Am. J. Sci.* **301**, 1–15.

Polissar P. J., Freeman K. H., Rowley D. B., McInerney F. A. and Currie B. S. (2009) Paleoaltimetry of the Tibetan Plateau from D/H ratios of lipid biomarkers. *Earth Planet. Sci. Lett.* **287**, 64–76.

Poulsen C. J., Ehlers T. A. and Insel N. (2010) Onset of convective rainfall during gradual late Miocene rise of the central Andes. *Science* **328**, 490–493.

Quade J., Breecker D. O., Daëron M. and Eiler J. (2011) The paleoaltimetry of Tibet: an isotopic perspective. *Am. J. Sci.* **311**, 77–115.

Quade J., Garzione C. and Eiler J. (2007) Paleoelevation reconstruction using pedogenic carbonates. *Rev. Mineral. Geochem.* **66**, 53.

Rohrmann A., Strecker M. R., Bookhagen B., Mulch A., Sachse D., Pingel H., Alonso R. N., Schildgen T. F. and Montero C. (2014) Can stable isotopes ride out the storms? The role of convection for water isotopes in models, records, and paleoaltimetry studies in the central Andes. *Earth Planet. Sci. Lett.* **407**, 187–195.

Rowley D. B. (2007) Stable isotope-based paleoaltimetry: theory and validation. *Rev. Mineral. Geochem.* **66**, 23–52.

Rowley D. B. and Garzione C. N. (2007) Stable isotope-based paleoaltimetry. *Annu. Rev. Earth Planet. Sci.* **35**, 463–508.

Rowley D. B., Pierrehumbert R. T. and Currie B. S. (2001) A new approach to stable isotope-based paleoaltimetry: implications for paleoaltimetry and paleohypsometry of the High Himalaya since the Late Miocene. *Earth Planet. Sci. Lett.* **188**, 253–268.

Rozanski K., Araguas-Araguas L. and Gonfiantini R. (1993) Isotopic patterns in modern global precipitation. *Clim. change Cont. Isot. Rec.* **78**, 1–36.

Salati E., Dall'Olio A., Matsui E. and Gat J. R. (1979) Recycling of water in the Amazon basin: an isotopic study. *Water Resour. Res.* **15**, 1250–1258.

Samuels-Crow K. E., Galewsky J., Hardy D. R., Sharp Z. D., Worden J. and Braun C. (2014a) Upwind convective influences on the isotopic composition of atmospheric water vapor over the tropical Andes. *J. Geophys. Res. Atmos.* **119**, 7051–7063.

Samuels-Crow K. E., Galewsky J., Sharp Z. D. and Dennis K. J. (2014b) Deuterium excess in subtropical free troposphere water vapor: continuous measurements from the Chajnantor Plateau, northern Chile. *Geophys. Res. Lett.* **41**, 8652–8659.

Saylor J. E. and Horton B. K. (2014) Nonuniform surface uplift of the Andean plateau revealed by deuterium isotopes in Miocene volcanic glass from southern Peru. *Earth Planet. Sci. Lett.* **387**, 120–131.

Saylor J. E., Quade J., Dettman D. L., DeCelles P. G., Kapp P. A. and Ding L. (2009) The late Miocene through present paleoelevation history of southwestern Tibet. *Am. J. Sci.* **309**(1), 1–42.

Sjostrom D. J. and Welker J. M. (2009) The influence of air mass source on the seasonal isotopic composition of precipitation, eastern USA. *J. Geochem. Explor.* **102**, 103–112.

Stewart M. K. (1975) Stable isotope fractionation due to evaporation and isotopic exchange of falling waterdrops: applications to atmospheric processes and evaporation of lakes. *J. Geophys. Res.* **80**, 1133–1146.

Takeuchi A. and Larson P. B. (2005) Oxygen isotope evidence for the late Cenozoic development of an orographic rain shadow in eastern Washington, USA. *Geology* **33**, 313–316.

Tian L., Masson-Delmotte V., Stievenard M., Yao T. and Jouzel J. (2001) Tibetan Plateau summer monsoon northward extent revealed by measurements of water stable isotopes. *J. Geophys. Res.* **106**, 28081–28088.

Tian L., Yao T., MacClune K., White J. W. C., Schilla A., Vaughn B., Vachon R. and Ichiyanagi K. (2007) Stable isotopic variations in west China: a consideration of moisture sources. *J. Geophys. Res. Series* **112**, 10112.

Trenberth K. E. (1999) Atmospheric moisture recycling: role of advection and local evaporation. *J. Clim.* **12**, 1368–1381.

Van der Ent R. J., Savenije H. H., Schaefli B. and Steele-Dunne S. C. (2010) Origin and fate of atmospheric moisture over continents. *Water Res. Res.* **46**.

Vuille M., Burns S., Taylor B., Cruz F., Bird B., Abbott M., Kanner L., Cheng H. and Novello V. (2012) A review of the South American monsoon history as recorded in stable isotopic proxies over the past two millennia. *Clim. Past* **8**, 1309–1321.

Vuille M. and Keimig F. (2004) Interannual variability of summertime convective cloudiness and precipitation in the central Andes derived from ISCCP-B3 data. *J. Clim.* **17**, 3334–3348.

Vuille M. and Werner M. (2005) Stable isotopes in precipitation recording South American summer monsoon and ENSO variability: observations and model results. *Clim. Dyn.* **25**, 401–413.

Yamada H. and Uyeda H. (2006) Transition of the rainfall characteristics related to the moistening of the land surface over the central Tibetan Plateau during the summer of 1998. *Mon. Weather Rev.* **134**, 3230–3247.

Yang M., Yao T., Gou X. and Tang H. (2007) Water recycling between the land surface and atmosphere on the Northern Tibetan Plateau – a case study at flat observation sites. *Arct. Antarct. Alp. Res.* **39**, 694–698.

Associate editor: Anthony Dosseto